

# Unsupervised Low-Light Image Enhancement Using Bright Channel Prior

Hunsang Lee , *Student Member, IEEE*, Kwanghoon Sohn , *Senior Member, IEEE*,  
and Dongbo Min , *Senior Member, IEEE*

**Abstract**—Recent approaches for low-light image enhancement achieve excellent performance through supervised learning based on convolutional neural networks. However, it is still challenging to collect a large amount of low-/normal-light image pairs in real environments for training the networks. In this letter, we propose an unsupervised learning approach for single low-light image enhancement using the bright channel prior (BCP) that the brightest pixel in a small patch is likely to be close to 1. An unsupervised loss function is defined with the pseudo ground-truth generated using the BCP. An enhancement network, consisting of a simple encoder-decoder, is then trained using the unsupervised loss function. To the best of our knowledge, this is the first attempt that enhances a low-light image through unsupervised learning. Furthermore, we introduce saturation loss and self-attention map for preserving image details and naturalness in the enhanced result. The performance of the proposed method is validated on various public datasets. Experimental results demonstrate that the proposed unsupervised approach achieves competitive performance over state-of-the-art methods based on supervised learning.

**Index Terms**—Unsupervised learning, low-light image enhancement, bright channel prior.

## I. INTRODUCTION

IMAGES acquired in the low-light environment are often degraded by poor visibility and low contrast. High-quality images can be obtained by increasing an exposure time, but this may incur blurs when a scene is not static. Over the past decades, various methods have been proposed to address this degradation that may dramatically deteriorate the performance of computer vision applications such as object detection [1] and recognition [2].

Early approaches attempted to enhance a dark areas by stretching the dynamic range of an input image histogram [3], [4], but

Manuscript received November 4, 2019; revised December 30, 2019; accepted January 2, 2020. Date of publication January 10, 2020; date of current version February 12, 2020. This work was supported by the Research Fund of Chungnam National University. This work was performed when Dongbo Min was with Chungnam National University. The associate editor coordinating the review of this manuscript and approving it for publication was Dr. Daniel P. K. Lun. (Corresponding author: Dongbo Min.)

H. Lee and K. Sohn are with the School of Electrical and Electronic Engineering, Yonsei University, Seoul 03722, South Korea (e-mail: hslee91@yonsei.ac.kr; khsohn@yonsei.ac.kr).

D. Min was with Chungnam National University, Daejeon 34134, South Korea. He is now with the Department of Computer Science and Engineering, Ewha Womans University, Seoul 03760, South Korea (e-mail: dbmin@ewha.ac.kr).

This article has supplementary downloadable material available at <https://ieeexplore.ieee.org>, provided by the authors.

Digital Object Identifier 10.1109/LSP.2020.2965824

such global operators often lead to a detail loss in the enhanced image. Zhang *et al.* [5] restrained noise by applying a joint-bilateral filter [6] after enhancing a low-light image. Retinex-based approaches [7]–[13] decompose an input image into reflectance and illumination components, and then simply consider the estimated reflectance map as an enhanced output or generate the result by manipulating the illumination. Wang *et al.* [9] obtained an enhanced image by applying joint edge-preserving filter to coarse illumination components. Fu *et al.* [10] explained the side effect of logarithmic transformation used in the Retinex model and addressed this issue with a weighted variable model to refine the regularization term. Guo *et al.* [11] predicted illumination component using structure-aware smoothing. Cai *et al.* [12] proposed a joint prior model with shape, illumination and texture assumption for better prior representation.

Recently, convolutional neural networks (CNN) have been applied to the low-light image enhancement [14]–[19], following the success in the field of image restoration including image denoising [20], super-resolution [21], rain streak removal [22], and haze removal [23]. Gharbi *et al.* [14] estimated an enhanced image by combining the bilateral grid algorithm [24] with local affine color transformation into deep networks. Lore *et al.* [15] used a stacked auto-encoder to sequentially perform the patch-based low-light enhancement and noise reduction. Li *et al.* [17] and Wang *et al.* [18] established the mapping relationship between the illumination maps of low- and normal-light images. Wei *et al.* [16] separated an input image into reflectance and illumination based on the Retinex model. After adjusting the brightness of the illumination map and applying denoising algorithm [25] to the reflectance image, an enhanced image is obtained by combining the two components. Ren *et al.* [19] enhanced visibility by estimating global content using CNN and refined image details using the spatially variant recurrent neural networks (RNN).

Generative adversarial networks (GAN) has also been used for low-light image enhancement [26]–[28]. Montulet *et al.* [26] used PatchGAN [29] to obtain enhanced results in a locally-adaptive manner instead of brightening an entire image. Jiang *et al.* [27] leveraged unpaired training data in order to match the intensity distribution of low-light images and (unpaired) normal-light images through PatchGAN [29]. Hu *et al.* [28] adopted the reinforcement learning guided by GAN to generate user-understandable operation sequences for photo retouching.

Though these learning-based methods outperform existing handcrafted low-light enhancement approaches thanks to its

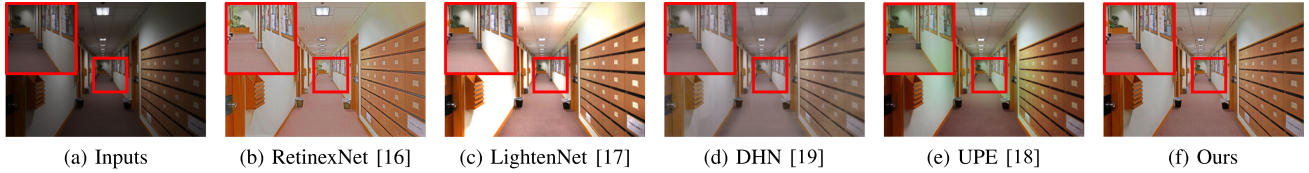


Fig. 1. Unnaturalness of existing methods. Best viewed in electronic version.

powerful representation learning, they still face several issues. They are mostly based on the supervised learning that requires a large-scale training data consisting of low-light images as inputs and normal images as ground-truth. It is, however, challenging to construct a large-scale training data that takes into account the real-world environment. For instance, it is relatively easy to obtain a pair of images with different exposures and then generate a high dynamic range (HDR) image as ground-truth [30], but it is possible only when the scene is static and is taken at daytime. Obtaining a large amount of clear normal light images in an extremely low-light environment is tremendously challenging. Lore *et al.* [15] synthesized training data by applying gamma correction to normal images. However, such a degradation is not realistic, and thus it is difficult to adapt the model trained with the synthetic training data to the real low-light image due to a large domain gap. Wang *et al.* [18] released a new training dataset for low light image enhancement. Normal images were captured by digital camera or collected from Flickr [31]. To generate low-light images, three experts retouched the normal images using Adobe Lightroom, similar to the MIT-Adobe FiveK dataset [32]. However, this is an expensive and labor-intensive task.

In addition, CNN-based approaches [16]–[19] often failed to yield visually natural results. For instance, as shown in Fig. 1, Some methods [16], [17] over-enhance low-light areas, producing unnatural results. Ren *et al.* [19] change a color tone of the input image globally. Wang *et al.* [18] often cause a color-inconsistency problem due to an incorrectly estimated illumination map and suffer from low-visibility.

To tackle the above-mentioned problems, we propose a novel unsupervised approach for the low-light image enhancement. Motivated by the dark channel prior (DCP) used in the haze removal [33], [34], we design the deep network that is trained using the bright channel prior (BCP) [35] with no normal image as ground-truth. The BCP imposes the constraint that the brightest pixel in a small patch of the enhanced image is close to 1. We utilize the BCP to generate an initial illumination map as pseudo ground-truth. To the best of our knowledge, this is the first attempt to enhance the low-light image through the unsupervised learning. Furthermore, we employ a saturation loss and a self-attention map to preserve an image naturalness even in the presence of bright regions in an low-light image. This enables the proposed network to avoid an over-saturation, while enhancing dark areas and preserving details in the resultant image. Main contributions are summarized as follows.

- We propose an unsupervised learning approach for the low-light image enhancement.
- Thanks to the saturation loss and self-attention map, our method preserves image details and naturalness in the enhanced images effectively.

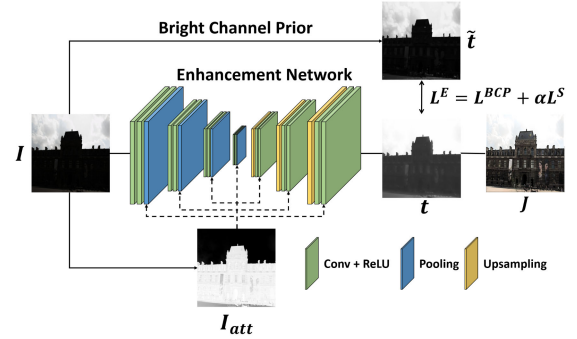


Fig. 2. The overall architecture of the proposed method.  $I_{att}$  and  $\tilde{t}$  are computed from an input image.

## II. PROPOSED METHOD

The proposed network consists of a simple encoder-decoder, as shown in Fig. 2. An initial illumination map  $\tilde{t}$  is first estimated by using the BCP [35], and this is then used to define an unsupervised loss function  $L^{BCP}$  for the enhancement network that estimates a final illumination map  $t$ . To deal with blocky artifacts in the initial illumination map, the regularization term of the soft-matting [36] is additionally used in  $L^{BCP}$ . The saturation loss  $L^S$  and self-attention map  $I_{att}$  are applied to deal with the over-saturation problem, making the enhanced image more natural and preserving image details. Note that different from recent approaches [14]–[19] based on complicated architectures, the proposed method employs the simple encoder-decoder only. Even with such a simple network, the proposed *unsupervised* method achieves a competitive performance over the recent *supervised* approaches.

### A. Initial Illumination Map Estimation

BCP [35] was proposed to adjust the local exposure of an image. This is a variant of dark channel prior (DCP) [33] originally proposed to predict the transmission map of an input haze image. We adopt the BCP for predicting an initial illumination map that is used to define the unsupervised loss in the proposed enhancement network. The low-light image model for the BCP is defined as follows:

$$I_p = t_p J_p + (1 - t_p) A, \quad (1)$$

where  $I_p$  and  $J_p \in \mathbb{R}^3$  represent an observed low-light image and an enhanced output image.  $t_p \in \mathbb{R}$  and  $A \in \mathbb{R}^3$  indicate an illumination map and an environment light, respectively. The brightest intensity within the patch  $\Omega(p)$  centered at the pixel  $p$



Fig. 3. Effect of the regularization term in Eq. (6). (a) initial illumination map with blocky artifacts. (b) predicted illumination map with  $L^{BCP}$ .

is defined as

$$J_p^{bright} = \max_{c \in r, g, b} \left( \max_{q \in \Omega(p)} J_q^c \right). \quad (2)$$

According to the BCP [35], the brightest intensity becomes  $J_p^{bright} \rightarrow 1$ . Under the assumption that  $A$  is known and the illumination map, denoted as  $\tilde{t}$ , is constant within  $\Omega(p)$ , we obtain the following equation by applying the max operator to both sides of Eq. (1):

$$\tilde{t}_p = 1 - \max_{c, q} \left( \frac{1 - I_q^c}{1 - A^c} \right). \quad (3)$$

The darkest pixel may be used as the environment light. However, it could be dark object or shadow in real environment. Thus, similar to [33],  $A$  is computed with a set of the darkest 0.1% pixels (denoted as  $K$ ) in the bright channel of  $I (= \max_{c \in r, g, b} I^c)$ :

$$A = \frac{1}{|K|} \sum_{p \in K} I_p. \quad (4)$$

### B. Unsupervised Estimation of Illumination Map

1) *Bright Channel Prior Loss*: The initial illumination map  $\tilde{t}$  serves as the supervision for training the proposed network. To be specific, the enhancement network in Fig. 2 produces the illumination map  $t$  with the supervision of  $\tilde{t}$ , and  $t$  is then used to generate the enhanced image as follows,

$$J_p = \frac{I_p - A}{t_p} + A. \quad (5)$$

However, since  $\tilde{t}$  is assumed to be constant within  $\Omega(p)$ , it often produces blocky artifacts, making the output image also blocky. Fig. 3(a) shows the blocky artifacts of the initial illumination map  $\tilde{t}$ . We address this issue by leveraging an additional regularizer for the unsupervised loss function used in [34]. Considering Eq. (1) is conceptually similar to the image matting [36] in which an output image is expressed as a linear combination of foreground and background, we adopt the regularizer of the soft matting [36]. The unsupervised loss function based on the BCP is finally defined as

$$L^{BCP} = \frac{1}{N} \sum_p \left\{ (t_p - \tilde{t}_p)^2 + \lambda \sum_{i, j \in \Psi(p)} w_{ij} (t_i - t_j)^2 \right\}, \quad (6)$$

where  $w_{ij}$  is the weight of the matting Laplacian matrix that computes affinity between  $I_i$  and  $I_j$ .  $\Psi(p)$  represents  $3 \times 3$  patch around center pixel  $p$ .  $N$  means the total number of pixels, and  $\lambda$  is a weight parameter that controls the balance between data term and smoothness term.

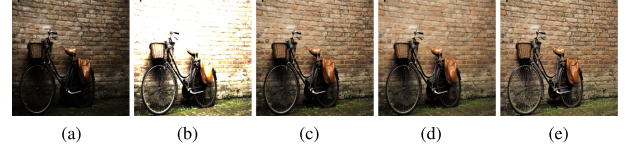


Fig. 4. Saturation suppression by saturation loss and self-attention map. Each image represents (a) input, (b) with  $L^{BCP}$ , (c) with  $L^{BCP}$  and  $I_{att}$ , (d) with  $L^{BCP}$  and  $L^S$ , (e) with  $L^{BCP}$ ,  $L^S$  and  $I_{att}$ . Best viewed in electronic version.

2) *Saturation Loss*: In Eq. (5), when  $t$  is too small, the output image  $J$  often exceeds the range of the color gamut  $[0, 1]$ . To address this issue, we define a lower bound of  $t_p$ , denoted as  $t_p^{\min} = \max_c \left( \frac{I_p^c - A^c}{1 - A^c} \right)$ , by formulating Eq. (5) with respect to  $t$  and applying the max operator over  $c$ . The saturation loss  $L_p^S$  is then defined for a pixel  $p$  as

$$L_p^S = \begin{cases} 0 & t_p \geq t_p^{\min} \\ (t_p - t_p^{\min})^2 & \text{otherwise} \end{cases}. \quad (7)$$

It can be simply defined using a saturation mask  $M_p$  as

$$L^S = \frac{1}{N} \sum_p \|M_p \cdot (t_p - t_p^{\min})\|_2, \quad (8)$$

where  $M_p = 0$  when  $t_p \geq t_p^{\min}$ , 1 otherwise. The saturation loss  $L^S$  enforces  $t_p$  to become close to  $t_p^{\min}$  when saturation occurs, i.e.,  $t_p < t_p^{\min}$ . The final loss function for the enhancement network is defined as follows:

$$L^E = L^{BCP} + \alpha L^S. \quad (9)$$

3) *Self-Attention Guided Enhancement*: Even though the saturation loss mitigates the over-saturation problem, it may still appear by other factors. We assume that  $A$  is constant over an entire image regardless of brightness, though it is computed as an average of pixels belonging to only dark regions in Eq. (4). Thus, when the enhancement network is applied to an image with a large variation of brightness, an over-saturation often appears in the bright regions of the input low-light image, e.g. sky and snow. One possible solution is to estimate a locally-varying environment light map using deep networks, but the unsupervised estimation of the environment light map poses additional challenges. Instead, inspired by [27], we propose to design a self-attention map on the HSV channel of the low-light image as

$$I_{att} = (1 - I^V)^\gamma, \quad (10)$$

where  $I^V$  is V channel of HSV image of  $I$ , since we consider only the brightness of the image.  $\gamma \geq 1$  is a parameter that controls the curvature of the attention map.  $I_{att}$  is multiplied to convolutional activations of all layers in the enhancement network  $E$ , as shown in Fig. 2. This enables for adapting the proposed network accordingly depending on the brightness of the image. Brighter regions are given lower weights to avoid over-saturation, while preserving image details and enhancing the contrast in the dark regions effectively. Fig. 4 shows the effectiveness of the saturation loss and self-attention map. They boost the performance while keeping image details and naturalness.

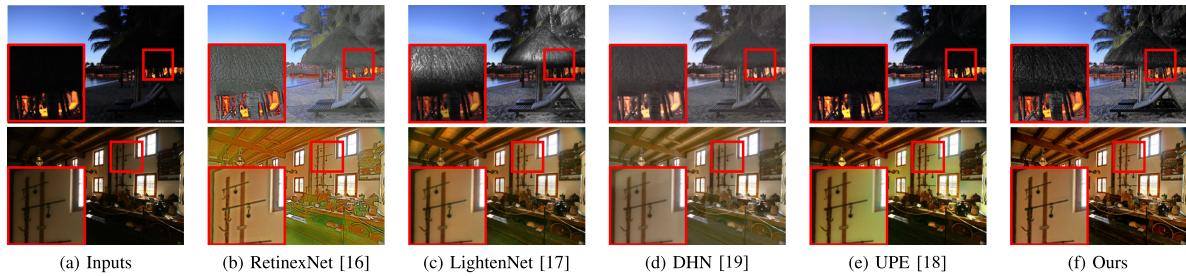


Fig. 5. Qualitative evaluation with state-of-the-art methods on test set. Best viewed in electronic version.

TABLE I  
EFFECT OF SATURATION LOSS AND SELF-ATTENTION MAP.  
THE LOWER IS THE BETTER

Method	Dataset			
	FiveK [32]	LIME [11]	NPE [9]	Avg.
	NIQE / LOE			
$L^{BCP}$	4.05 / 751	4.50 / 506	5.27 / 1329	4.22 / 823
$L^{BCP} + L^S$	3.44 / 394	3.87 / 270	3.22 / 335	3.33 / 384
$L^{BCP} + I_{att}$	3.41 / 417	3.83 / 321	3.53 / 332	3.55 / 404
$L^{BCP} + L^S + I_{att}$	<b>3.35 / 303</b>	<b>3.78 / 209</b>	<b>3.18 / 327</b>	<b>3.30 / 305</b>

### III. EXPERIMENTAL RESULTS

#### A. Experimental Settings

Since the proposed method is based on the unsupervised learning, any low-light images can be used for training. We collected the training data from several publicly available datasets such as LOL [16] and SICE [37]. LOL dataset [16] provides 1500 low/normal-light synthetic image pairs. SICE dataset [37] provides multi-exposure sequences and corresponding HDR images of 589 scenes. For training/validation split, 1485 images of LOL and 534 images of SICE are used for training and the rest is used for validation. Following state-of-the-art method, UPE [18], we conducted the performance evaluation with 500 images of MIT-Adobe FiveK dataset [32]. In addition, LIME [11], NPE [9] and MEF [38] datasets were also used for an extensive comparison.

Our network was trained with Adam optimizer, the learning rate was  $10^{-3}$  at first and linearly decreased by  $10^{-5}$  until 50 epochs. For data augmentation, we adopted random cropping, rotation and flipping. The patch size of  $\Omega$  and  $\Psi$  were  $15 \times 15$  and  $3 \times 3$ .  $\lambda$  and  $\gamma$  were set to 0.1 and 2.5.  $\alpha$ , which adjust the balance between two loss terms, was set to 0.1.

#### B. Quantitative Results

We adopted two no-reference metrics widely used in low-light image enhancement for performance evaluation: naturalness image quality evaluator (NIQE) [39] and lightness order error (LOE) [9], which measure the image naturalness and the lightness distortion, respectively. We first performed an ablation study of the proposed components in Table I. The saturation loss and self-attention map progressively improve the performance of the proposed method. This is also consistent with the visual comparison of Fig. 4. Table II shows the quantitative results on FiveK [32], LIME [11] and NPE [9] datasets. Note that, four approaches [16]–[19] are based on supervised learning and LIME [11] is a handcrafted approach. The numbers with bold, red and blue indicate the 1<sup>st</sup>, 2<sup>nd</sup> and 3<sup>rd</sup> results, respectively.

TABLE II  
QUANTITATIVE EVALUATION USING NO-REFERENCE IMAGE QUALITY  
EVALUATORS. THE LOWER IS THE BETTER

Method	Dataset			
	FiveK [32]	LIME [11]	NPE [9]	Avg.
	NIQE / LOE			
RetinexNet [16]	4.26 / 2125	4.75 / 1518	4.39 / 1675	4.34 / 1907
LightenNet [17]	3.40 / 2378	<b>3.49</b> / 1914	3.22 / 1403	3.33 / 1952
LIME [11]	3.49 / 1203	4.25 / <b>1134</b>	3.53 / 1241	3.55 / 1215
DHN [19]	<b>3.29</b> / <b>369</b>	<b>3.59</b> / <b>374</b>	<b>3.16</b> / <b>511</b>	<b>3.25</b> / <b>428</b>
UPE [18]	<b>3.23</b> / <b>1003</b>	3.92 / 1237	<b>2.98</b> / <b>796</b>	<b>3.16</b> / <b>930</b>
Ours	<b>3.35</b> / <b>303</b>	<b>3.78</b> / <b>209</b>	<b>3.18</b> / <b>327</b>	<b>3.30</b> / <b>305</b>

The proposed method achieves comparable results to UPE [18] and DHN [19] on the NIQE [39], and outperforms them on the LOE [9].

#### C. Qualitative Results

We qualitatively evaluated the proposed method in Fig. 5. Only the results of some images in NPE [9] and MEF [38] datasets are shown due to a page limit. More results are provided in the supplementary material. The RetinexNet [16] and the LightenNet [17] over-enhance input images, making enhanced results unnatural. The DHN [19] often loses image details, and thus the results do not contain vivid and natural color. The results of UPE [18] are more natural compared to other methods, but there is still a color-inconsistency problem in some images. For example, in the second row image, the color of wall was distorted into green. Contrarily, our method preserves image details and naturalness well and maintains the color consistency, while enhancing dark regions effectively.

### IV. CONCLUSION

In this letter, we have proposed a new unsupervised learning approach for low-light image enhancement. By making use of the unsupervised loss based on the BCP, we addressed the difficulty of constructing a large-scale training data with ground-truth required to train deep networks for low-light enhancement. Additionally, thanks to the self-attention map and saturation loss, the image details and naturalness are preserved well in the enhanced images. Although our network is trained without ground-truth data, it has been demonstrated to be competitive over state-of-the-art supervised approaches through quantitative and qualitative comparisons. As future work, since a low-light image often contains noise, we plan to develop a new network that handles amplified noise in the enhanced images.

## REFERENCES

- [1] J. Redmon, S. Divvala, R. Girshick, and A. Farhadi, "You only look once: Unified, real-time object detection," in *Proc. IEEE Conf. Comput. Vision Pattern Recognit.*, 2016, pp. 779–788.
- [2] J. Deng, W. Dong, R. Socher, L.-J. Li, K. Li, and L. Fei-Fei, "Imagenet: A large-scale hierarchical image database," in *Proc. IEEE Conf. Comput. Vision Pattern Recognit.*, 2009, pp. 248–255.
- [3] S. M. Pizer, R. E. Johnston, J. P. Ericksen, B. C. Yankaskas, and K. E. Muller, "Contrast-limited adaptive histogram equalization: Speed and effectiveness," in *Proc. IEEE Conf. Visualization Biomed. Comput.*, 1990, pp. 337–345.
- [4] M. Abdullah-Al-Wadud, M. H. Kabir, M. A. A. Dewan, and O. Chae, "A dynamic histogram equalization for image contrast enhancement," *IEEE Trans. Consum. Electron.*, vol. 53, no. 2, pp. 593–600, May 2007.
- [5] X. Zhang, P. Shen, L. Luo, L. Zhang, and J. Song, "Enhancement and noise reduction of very low light level images," in *Proc. Int. Conf. Pattern Recognit.*, 2012, pp. 2034–2037.
- [6] G. Petschnigg, R. Szeliski, M. Agrawala, M. Cohen, H. Hoppe, and K. Toyama, "Digital photography with flash and no-flash image pairs," *ACM Trans. Graph.*, vol. 23, no. 3, pp. 664–672, 2004.
- [7] D. J. Jobson, Z.-U. Rahman, and G. A. Woodell, "Properties and performance of a center/surround retinex," *IEEE Trans. Image Process.*, vol. 6, no. 3, pp. 451–462, Mar. 1997.
- [8] D. J. Jobson, Z.-u. Rahman, and G. A. Woodell, "A multiscale retinex for bridging the gap between color images and the human observation of scenes," *IEEE Trans. Image Process.*, vol. 6, no. 7, pp. 965–976, Jul. 1997.
- [9] S. Wang, J. Zheng, H.-M. Hu, and B. Li, "Naturalness preserved enhancement algorithm for non-uniform illumination images," *IEEE Trans. Image Process.*, vol. 22, no. 9, pp. 3538–3548, Sep. 2013.
- [10] X. Fu, D. Zeng, Y. Huang, X.-P. Zhang, and X. Ding, "A weighted variational model for simultaneous reflectance and illumination estimation," in *Proc. IEEE Conf. Comput. Vision Pattern Recognit.*, 2016, pp. 2782–2790.
- [11] X. Guo, Y. Li, and H. Ling, "Lime: Low-light image enhancement via illumination map estimation," *IEEE Trans. Image Process.*, vol. 26, no. 2, pp. 982–993, Feb. 2016.
- [12] B. Cai, X. Xu, K. Guo, K. Jia, B. Hu, and D. Tao, "A joint intrinsic-extrinsic prior model for retinex," in *Proc. IEEE Int. Conf. Comput. Vision*, 2017, pp. 4000–4009.
- [13] Q. Zhang, G. Yuan, C. Xiao, L. Zhu, and W.-S. Zheng, "High-quality exposure correction of underexposed photos," in *Proc. ACM Int. Conf. Multimedia*, 2018, pp. 582–590.
- [14] M. Gharbi, J. Chen, J. T. Barron, S. W. Hasinoff, and F. Durand, "Deep bilateral learning for real-time image enhancement," *ACM Trans. Graph.*, vol. 36, no. 4, p. 118, 2017.
- [15] K. G. Lore, A. Akitayo, and S. Sarkar, "LLNET: A deep autoencoder approach to natural low-light image enhancement," *Pattern Recognit.*, vol. 61, pp. 650–662, 2017.
- [16] C. Wei, W. Wang, W. Yang, and J. Liu, "Deep retinex decomposition for low-light enhancement," in *Proc. Brit. Mach. Vision Conf.*, 2018, pp. 1–12.
- [17] C. Li, J. Guo, F. Porikli, and Y. Pang, "LightenNet: A convolutional neural network for weakly illuminated image enhancement," *Pattern Recognit. Lett.*, vol. 104, pp. 15–22, 2018.
- [18] R. Wang, Q. Zhang, C.-W. Fu, X. Shen, W.-S. Zheng, and J. Jia, "Underexposed photo enhancement using deep illumination estimation," in *Proc. IEEE Conf. Comput. Vision Pattern Recognit.*, 2019, pp. 6849–6857.
- [19] W. Ren *et al.*, "Low-light image enhancement via a deep hybrid network," *IEEE Trans. Image Process.*, vol. 28, no. 9, pp. 4364–4375, Sep. 2019.
- [20] K. Zhang, W. Zuo, Y. Chen, D. Meng, and L. Zhang, "Beyond a Gaussian denoiser: Residual learning of deep CNN for image denoising," *IEEE Trans. Image Process.*, vol. 26, no. 7, pp. 3142–3155, Jul. 2017.
- [21] C. Dong, C. C. Loy, K. He, and X. Tang, "Image super-resolution using deep convolutional networks," *IEEE Trans. Pattern Anal. Mach. Intell.*, vol. 38, no. 2, pp. 295–307, Feb. 2016.
- [22] X. Fu, J. Huang, X. Ding, Y. Liao, and J. Paisley, "Clearing the skies: A deep network architecture for single-image rain removal," *IEEE Trans. Image Process.*, vol. 26, no. 6, pp. 2944–2956, Jun. 2017.
- [23] W. Ren, S. Liu, H. Zhang, J. Pan, X. Cao, and M.-H. Yang, "Single image dehazing via multi-scale convolutional neural networks," in *Proc. Euro. Conf. Comput. Vision*, 2016, pp. 154–169.
- [24] J. Chen, S. Paris, and F. Durand, "Real-time edge-aware image processing with the bilateral grid," *ACM Trans. Graph.*, vol. 26, no. 3, 2007, Art. no. 103.
- [25] K. Dabov, A. Foi, V. Katkovnik, and K. Egiazarian, "Image denoising by sparse 3-D transform-domain collaborative filtering," *IEEE Trans. Image Process.*, vol. 16, no. 8, pp. 2080–2095, Aug. 2007.
- [26] R. Montulet, A. Briassouli, and N. Maastricht, "Deep learning for robust end-to-end tone mapping," in *Proc. Brit. Mach. Vision Conf.*, 2019, pp. 1–12.
- [27] Y. Jiang *et al.*, "Enlightengan: Deep light enhancement without paired supervision," 2019, *arXiv:1906.06972*.
- [28] Y. Hu, H. He, C. Xu, B. Wang, and S. Lin, "Exposure: A white-box photo post-processing framework," *ACM Trans. Graph.*, vol. 37, no. 2, p. 26, 2018.
- [29] P. Isola, J.-Y. Zhu, T. Zhou, and A. A. Efros, "Image-to-image translation with conditional adversarial networks," in *Proc. IEEE Conf. Comput. Vision Pattern Recognit.*, 2017, pp. 1125–1134.
- [30] A. A. Goshtasby, "Fusion of multi-exposure images," *Image Vision Comput.*, vol. 23, no. 6, pp. 611–618, 2005.
- [31] Flickr web site. 2018. [Online]. Available: <https://www.flickr.com/>
- [32] V. Bychkovsky, S. Paris, E. Chan, and F. Durand, "Learning photographic global tonal adjustment with a database of input/output image pairs," in *Proc. IEEE Conf. Comput. Vision Pattern Recognit.*, 2011, pp. 97–104.
- [33] K. He, J. Sun, and X. Tang, "Single image haze removal using dark channel prior," *IEEE Trans. Pattern Anal. Mach. Intell.*, vol. 33, no. 12, pp. 2341–2353, Dec. 2011.
- [34] A. Golts, D. Freedman, and M. Elad, "Unsupervised single image dehazing using dark channel prior loss," *IEEE Trans. Image Process.*, vol. 29, pp. 2692–2701, 2020.
- [35] Y. Wang, S. Zhuo, D. Tao, J. Bu, and N. Li, "Automatic local exposure correction using bright channel prior for under-exposed images," *Signal Process.*, vol. 93, no. 11, pp. 3227–3238, 2013.
- [36] A. Levin, D. Lischinski, and Y. Weiss, "A closed-form solution to natural image matting," *IEEE Trans. Pattern Anal. Mach. Intell.*, vol. 30, no. 2, pp. 228–242, Feb. 2008.
- [37] J. Cai, S. Gu, and L. Zhang, "Learning a deep single image contrast enhancer from multi-exposure images," *IEEE Trans. Image Process.*, vol. 27, no. 4, pp. 2049–2062, Apr. 2018.
- [38] K. Ma, K. Zeng, and Z. Wang, "Perceptual quality assessment for multi-exposure image fusion," *IEEE Trans. Image Process.*, vol. 24, no. 11, pp. 3345–3356, Nov. 2015.
- [39] A. Mittal, R. Soundararajan, and A. C. Bovik, "Making a 'completely blind' image quality analyzer," *IEEE Signal Process. Lett.*, vol. 20, no. 3, pp. 209–212, Mar. 2013.